


# Electromagnetic Force Analysis of a Power Transformer Under the Short-Circuit Condition

Yi Li, Qiuyuan Xu, and Yanfeng Lu 

**Abstract**—Due to the high costs and difficulties to make the short-current experiment of large power transformers, it is critical to do the electromagnetic force analysis of the transformer windings through finite element software. Research in this paper establishes the analysis model of a 50000 KVA/110 KV three phase power transformer. In previous studies, short-circuit impedance is seldom evaluated for its effect to the accumulated effect of the electromagnetic force. A novel approach with considering of the short-circuit impedance is proposed to simulate the accumulated deformation. Short-circuit current is applied to this model, testing the electromagnetic forces of the transformer windings. Results of the research is significant to the evaluation of winding deformation state.

**Index Terms**—Electromagnetic forces, electromagnetic fields, finite element analysis, power transformers.

## I. INTRODUCTION

AS one of the common electrical devices in the power system, power transformer undertakes the important tasks of changing AC voltage. When short-circuit faults occur, huge short-circuit electromagnetic force can be exerted on transformer windings, resulting in deformation or even damage to the winding, which will cause safety hazards to the grid.

According to the electromagnetic field theory, power transformer windings which conduct electricity will produce electromagnetic field in space, leading to electromagnetic force on the conducting windings. When short-circuit fault occurs, especially the three phase grounding one, the current can rise to several times or even dozens of times of the normal value. It will cause hundred or even thousand times electromagnetic force, sometimes leading to the extreme condition like winding collapse. In the previous studies, for the convenience to analyze, this electromagnetic force under short-circuit faults is usually decomposed

to be axial and radial direction [1]. The radial part can lead to severe deformation of windings, which causes instability in radial direction, break the insulation material of the windings, lead to inter-turn faults, or even fire hazard. The axial part might causes vibration in axial direction, lead to winding collapse. When it comes to calculation of the magnetic force/torque, which is the important topic in both electrical machines and transformers, it is more cost-effective by building the simulation model instead of conduction the real test [2], [3]. Recently, the transformer modeling is researched widely to investigate the transient characteristics produced by over-voltage and the mechanical failures produced by impacts of short-circuit current in transformer windings, such as: multi-conductor transmission line model [4], [5], finite element model [6]–[8], and equivalent circuit model [9]. Among them, finite element model is mainly used to calculate and analyze the electromagnetic force. In this paper we present a three dimensional model of an 110 kV power transformer. We use this model to research the linkage between the electromagnetic force and impacts of short-circuit current. There are three windings (which are high, low and the regulated voltage windings) in this three phase transformer, as presented in Fig. 1. We conducted several simulation process of the three-phase short-circuit faults. It is because the peak current value of three-phase short-circuits is the maximum among that of all the faults. We also conducted simulation experiments to study the accumulated effect of the electromagnetic force. Seven times of short-circuit accidents are exerted to the windings. Here we propose an improved method by considering the effect of short-circuit impedance. Because once the deformation occurs, short-circuit impedance value will change.

In previous paper, conventionally, the maximum short-circuit current value stay same during the test. Therefore more precise results of the deformation data can be obtained if the influence of short-circuit impedance variation is considered.

## II. THEORETICAL ANALYSIS OF MODELING

Among several kinds of short-circuit faults, the three phases fault is the most serious one, for its current magnitude will be the highest. Moreover, which moment that short fault occurs also determines the current magnitude that can reach. Since the most severe condition will determine the final insulation and design parameters will choose, here we only consider the occasion where the highest short circuit current will take place. Through some analytic derivation, we know it is the zero-crossing time of AC voltage. Fig. 2 is a picture of three phase short fault current (high voltage side) under the mentioned condition. The expression of short-circuit fault current (phase A) can be expressed as

Manuscript received March 15, 2021; revised June 1, 2021 and July 27, 2021; accepted August 10, 2021. Date of publication August 25, 2021; date of current version September 22, 2021. This work was supported in part by the National Key Research and Development Plan of China under Grant 2020AAA0105900, in part by Sanbian Technology Corporation under program HL20190617110624000016, and in part by the open research fund of the State Key Laboratory for Management and Control of Complex Systems. (*Corresponding author: Yanfeng Lu.*)

Yi Li is with the School of Information Engineering, Nanchang University, Nanchang 330000, JiangXi, China (e-mail: littlepear@ncu.edu.cn).

Qiuyuan Xu is with the Sanbian Technology Corporation, Taizhou, Zhejiang 94720-8203, China (e-mail: xqyxqy6707@126.com).

Yanfeng Lu is with the State Key Laboratory of Management and Control for Complex Systems, Institute of Automation, Chinese Academy of Science, Beijing 100190, China (e-mail: yanfeng.lv@ia.ac.cn).

Color versions of one or more figures in this article are available at <https://doi.org/10.1109/TASC.2021.3107799>.

Digital Object Identifier 10.1109/TASC.2021.3107799

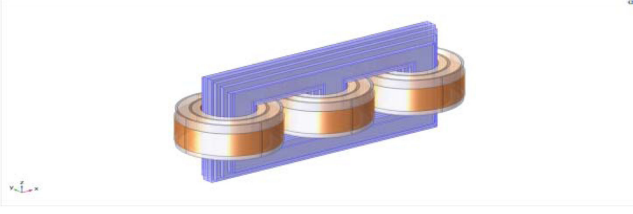


Fig. 1. Three dimensional simplified mode of transformer.

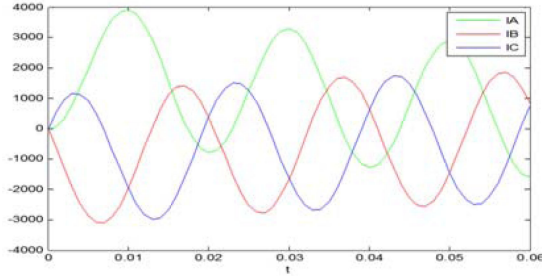


Fig. 2. Transient short circuit current under severest fault condition.

follows:

$$i_A = I_m [\sin(\omega t + \phi_A) - e^{-t/T_a} \sin \phi_A] \quad (1)$$

where  $I_m$  is the maximum value,  $\omega$  is angular frequency which is 314 rad/s here,  $\phi_A$  is the phase angle which is  $-\pi/2$  and  $T_a$  is a time constant which is 0.045.

On the basis of Lorentz law, the electromagnetic volume force can be expressed by the equation as follows:

$$f = J \times B \quad (2)$$

where  $J$  is the electromagnetic force per volume,  $J$  denotes the current density, and  $B$  denotes the magnetic flux density.

As shown in (1), the current density and magnetic flux density contributes to the electromagnetic force. These two kinds of densities vary with the time. On the other hand, according to Maxwell equation, the current also control the electromagnetic field, which can be described by the equation below:

$$\nabla^2 A = -\mu J \quad (3)$$

where  $\mu$  denotes the permeability of electromagnetic field,  $A$  is the magnetic vector potential. The relationship between magnetic flux density and magnetic vector potential can be derived as:

$$B_r = -\partial A / \partial z \quad (4)$$

$$B_z = \partial (rA) / r \partial r \quad (5)$$

where  $B_r$  is the magnetic flux density in radial direction and  $B_z$  is the magnetic flux density in axis direction.

These equations can be calculated by finite element method. The variation of short-circuit impedance will also take effect in the magnitude of the short-circuit current. In our simulation of the accumulated effect, we take this factor into account and evaluate the short-circuit impedance in different winding deformation state.

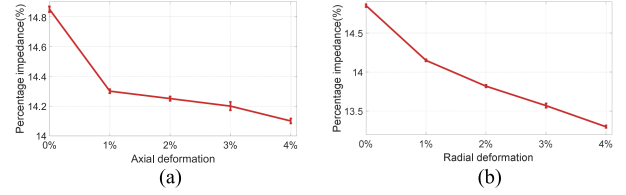


Fig. 3. (a) percentage impedance versus axial and radial deformations.

Here we get the short-circuit impedance by calculating the magnetic field energy. The detailed procedure is summarized as follows:

Step1: calculating the short-circuit impedance in different winding deformation state by the equations below.

Winding inductance can be expressed by the equation as follows:

$$W_m = \frac{1}{2} L I_k^2 \quad (6)$$

Where the  $W_m$  is the magnetic field energy,  $L$  is the winding inductance,  $I_k$  is the phase current. The relationship between leakage reactance and the magnetic field energy can be expressed as follows:

$$X_k = 4\pi f \frac{W_m}{I_k^2} \quad (7)$$

Where  $X_k$  is the leakage reactance and  $f$  is the AC frequency.

Because the resistive component of the short-circuit impedance can be neglected, leakage reactance can be approximately equal to short-circuit impedance. Therefore, the percentage short-circuit impedance can be expressed as:

$$U_k \% = \frac{X_k I_k}{U_k} \times 100\% \quad (8)$$

Where  $U_k$  is the phase voltage,  $U_k \%$  is the percentage impedance.

Step2: According to the relationship between short-circuit current and percentage short-circuit impedance, calculating the short-circuit current under various winding deformation state.

Fig. 3 are the connected line graphs of the percentage impedance versus axial and radial deformation. Fig. 3(a) illustrates the condition that windings move in axial direction because of the electromagnetic force under three-phase short-current fault. Based on the data in the graph it can be concluded that percentage impedance will decrease with the increasing distance of the axial movement. The similar property also applies to the relationship between percentage impedance versus radial deformation, as shown in Fig. 3(b).

Therefore the modified percentage impedance is applied in the simulation test where the accumulated effect of the electromagnetic force in short-circuit faults is studied. In the test the magnitude of short-circuit current is adjusted according to the varied percentage impedance. More accurate results of the accumulated effect exposed on the power transformer windings can be achieved. In the next section of this paper we demonstrate the results of the simulation test and compared the resulted data of our improved method and the traditional one.

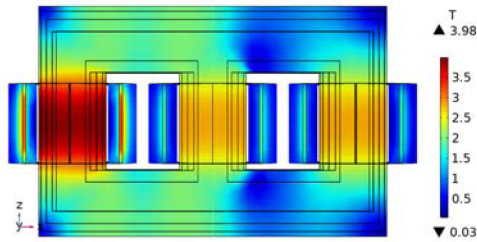


Fig. 4. Electromagnetic field distribution with principal tapping.

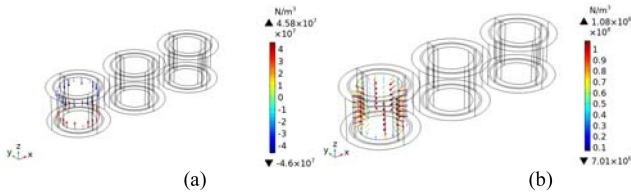


Fig. 5. (a) Axial direction force distribution of low voltage windings with principal tapping and (b) radial direction force distribution of low voltage windings with principal tapping.

 TABLE I  
 MAXIMUM VALUE OF AXIAL DIRECTION FORCE WITH PRINCIPAL TAPPING

Winding	Analytical(N/m <sup>3</sup> )	FEM(N/m <sup>3</sup> )	Error
HV	$7.780 \times 10^6$	$7.270 \times 10^6$	7%
LV	$4.855 \times 10^7$	$4.580 \times 10^7$	6%

### III. SIMULATION RESULTS

The electromagnetic forces is finally calculated by COMSOL, considering all three types of winding connections, namely maximum tapping, principal tapping and the minimum tapping. Fig. 4 illustrates the front view of transformer's magnetic field distribution at 0.01 seconds (when the short current at the peak value) with the principal tapping. It shows the maximum flux density occurring in A phase, where the short current reaches its peak.

For better analyzing, the winding's electromagnetic forces decomposed into two directions: axial and radial. Fig. 5(a) demonstrates the axial electromagnetic force of low voltage windings under principal tapping. It can be seen that the axial forces are mainly distributed in upper and bottom edge, and the direction of them are opposites. We also compared the results of using our finite element methods with using the newton analytical method [10], as shown in Table I. It is obvious that results through our model are quite close to that of the analytical method.

The right graph in Fig. 5(b) is plotted for demonstrating the axial force distributed under the same condition. It can be concluded that the largest radial direction force happens in the middle position of the windings, while in the upper and bottom edge it is relatively small.

The experiment of accumulated effect by considering the percentage impedance is conducted in two groups. One uses improved method fulfilled by the deformed geometry function in COMSOL while the other uses the conventional style for comparison. Table II demonstrates the resulted data. It can be

 TABLE II  
 MAXIMUM DEFORMATION OF LOW VOLTAGE WINDING

Short circuit times	Maximum Deformation/m	Maximum Deformation considering the Percentage Impedance/m
1	$1.690 \times 10^{-4}$	$1.690 \times 10^{-4}$
2	$1.865 \times 10^{-4}$	$1.869 \times 10^{-4}$
3	$2.741 \times 10^{-4}$	$2.754 \times 10^{-4}$
4	$1.650 \times 10^{-3}$	$1.665 \times 10^{-3}$
5	$1.489 \times 10^{-2}$	$1.506 \times 10^{-2}$
6	$6.613 \times 10^{-2}$	$6.692 \times 10^{-2}$
7	$2.967 \times 10^{-1}$	$3.004 \times 10^{-1}$

seen that for the low voltage side, when in the 6<sup>th</sup> accident, the difference is 0.79 mm which is small while in the 7<sup>th</sup> accidents, the difference can be as large as 3.7 mm, which is significant. It means when the number of short circuit faults increase, the accuracy of maximum deformation will be better when the percentage impedance is taken into consideration.

### IV. CONCLUSION

A model of 110 KV power transformer is established. Electromagnetic fields and forces of the transformer windings during three phase grounding faults are studied. An improved method that considering the short-circuit impedance is proposed. In the future we will focus on improve the accuracy of the model and study the material effects that might influence the electromagnetic force and the deformation.

### REFERENCES

- [1] H. Ahn, Y. Oh, J. Kim, J. Song, and S. Hahn, "Experimental verification and finite element analysis of short-circuit electromagnetic force for dry-type transformer," *IEEE Trans. Magn.*, vol. 48, no. 2, Feb. 2012, Art. no. 6136629.
- [2] X. Sun, Z. Jin, Y. Cai, Z. Yang, and L. Chen, "Grey wolf optimization algorithm based state feedback control for a bearingless permanent magnet synchronous machine," *IEEE Trans. Power Electron.*, vol. 35, no. 12, Dec. 2020, Art. no. 9091948.
- [3] X. Sun, Z. Jin, and L. Chen, and Z. Yang, "Disturbance rejection based on iterative learning control with extended state observer for a four-degree-of-freedom hybrid magnetic bearing system," *Mech. Syst. Signal Process.*, vol. 153, no. 3, May 2021, Art. no. 107465.
- [4] J. Zhang, W. Xu, C. Gao, and S. Wang, "Analysis of Inter-turn insulation of high voltage electrical machine by using multi-conductor transmission line model," *IEEE Trans. Magn.*, vol. 49, no. 5, May 2013, Art. no. 6514745.
- [5] Q. Zhang, S. Wang, and J. Qiu, "Application of an improved multiconductor transmission line model in power transformer," *IEEE Trans. Magn.*, vol. 49, no. 5, May 2013, Art. no. 6514602.
- [6] H. Wang and K. L. Butler, "Finite element analysis of internal winding faults in distribution transformers," *IEEE Trans. Power Del.*, vol. 16, no. 3, Mar. 2001, Art. no. 924821.
- [7] S. Liu, Z. Liu, and O. A. Mohammed, "FE-based modeling of single-phase distribution transformers with winding short circuit faults," *IEEE Trans. Magn.*, vol. 43, no. 4, Apr. 2007, Art. no. 4137814.
- [8] H. Zhang, S. Wang, S. Wang, H. Li, and D. Yuan, "Cumulative deformation analysis for transformer winding under short-circuit fault using magnetic-structural coupling model," *IEEE Trans. Appl. Supercond.*, vol. 26, no. 7, Oct. 2016, Art. no. 0606605.
- [9] B. Mork, F. Gonzalez, and D. Ishchenko, "Hybrid transformer model for transient simulation—Part I development and parameters," *IEEE Trans. Power Del.*, vol. 22, no. 1, Jan. 2007, Art. no. 4039455.
- [10] K. Dawood, M. A. Cinar, B. Alboyaci, and O. Sonmez, "Modelling and analysis of transformer using numerical and analytical methods," in *Proc. 18th Int. Symp. Electromagn. Fields Mechatronics Elect. Electron. Eng. Book Abstr.*, 2017, Art. no. 809069.